



Cite this: *J. Mater. Chem. B*, 2023,  
11, 5378

Received 3rd December 2022,  
Accepted 3rd February 2023

DOI: 10.1039/d2tb02643k

rsc.li/materials-b

## Nanotubes and water-channels from self-assembling dipeptides

Ottavia Bellotto, <sup>a</sup> Paola D'Andrea, <sup>b</sup> and Silvia Marchesan, <sup>\*ac</sup>

Dipeptides are attractive building blocks for biomaterials in light of their inherent biocompatibility, biodegradability, and simplicity of preparation. Since the discovery of diphenylalanine (Phe-Phe) self-assembling ability into nanotubes, research efforts have been devoted towards the identification of other dipeptide sequences capable of forming these interesting nanomorphologies, although design rules towards nanotube formation are still elusive. In this review, we analyze the dipeptide sequences reported thus far for their ability to form nanotubes, which often feature water-filled supramolecular channels as revealed by single-crystal X-ray diffraction, as well as their properties, and their potential biological applications, which span from drug delivery and regenerative medicine, to bioelectronics and bioimaging.

### 10th Anniversary Statement

Nanotubes formed by minimalistic dipeptides have been raising researchers' interest, not only for their inherent biocompatibility and biodegradability, but also for their emerging electronic properties. These nanotubes are being explored for diverse applications in light of their benign nature in terms of environmental impact. The roles of water in their inner cavities, and its impact on their physico-chemical properties, are a hot area of research. Our laboratories (<https://www.marchesanlab.com>) were opened in 2015, thanks to a starting grant on heterochiral tripeptides' self-assembly and their design based on the introduction of *D*-amino acids at selected positions to modulate the resulting supramolecular nanostructures and materials. The same year, we reported in *J. Mater. Chem. B* our research demonstrating that a simple shift in the positioning of the *D*-stereoconfiguration along a tripeptide was sufficient to change the level of supramolecular order of the assemblies, hence, the physicochemical properties of the resulting hydrogels, and their rates of enzymatic hydrolysis to modulate their biodegradation. In 2020, Prof. Marchesan joined the Advisory Board of *J. Mater. Chem. B*, which offers an ideal platform for research on materials derived from, and inspired by, biomolecules for a range of applications that go well beyond medicine.

<sup>a</sup> Chem. Pharm. Sc. Dept., University of Trieste, Via Giorgieri 1, 34127 Trieste, Italy. E-mail: smarchesan@units.it

<sup>b</sup> Life Sc. Dept., University of Trieste, Via Weiss 2, 34128 Trieste, Italy

<sup>c</sup> INSTM, Unit of Trieste, Via Giorgieri 1, 34127 Trieste, Italy



Ottavia Bellotto

Dr Ottavia Bellotto is a researcher at Dr Schär R&D center in Area Science Park (Trieste, Italy). In 2022, she was awarded her PhD in Chemistry with honours from the University of Trieste, supervised by Prof. Silvia Marchesan. Her doctoral research focussed on the design of self-assembling dipeptides for the development of nanotubes and hydrogel biomaterials. In 2018, she secured a 6-month fellowship funded by the National Cancer Institute (CRO) to develop biosensors based on antibodies and aptamers for Therapeutic Drug Monitoring. In 2017, she obtained her Master's degree in Medicinal Chemistry (University of Trieste), and she qualified as Pharmacist.



Paola D'Andrea

Prof. Paola D'Andrea is Associate Professor of Biochemistry at the University of Trieste, Department of Life Sciences. She carried out postdoctoral research at the Trinity College of Dublin (Ireland), at the Neuroscience Institute of the CNR in Milan, at the Department of Biotechnology (DIBIT) of the San Raffaele Hospital in Milan. She was visiting scientist at the Babraham Institute in Cambridge (UK) and at the Institut Pasteur of Paris (France). Her research

activity has focused on the mechanisms of calcium signalling, on gap junctions in genetic diseases, and on cellular modifications induced by tailored biointerfaces mimicking the extracellular matrix.

## Introduction

The most widely known nanotubes (NTs) are certainly carbon nanotubes, which, since their discovery by Iijima in 1991,<sup>1</sup> have attracted great interest especially for their electronic properties towards advanced applications in areas as diverse as tissue engineering,<sup>2–4</sup> energy<sup>5,6</sup> and catalysis,<sup>7,8</sup> conductive materials,<sup>9</sup> and electrodes for interfacing with biological tissues.<sup>10</sup> Besides inorganic alternatives,<sup>11</sup> such as boron nitride<sup>12</sup> and metal chalcogenides,<sup>13</sup> peptide-based organic NTs are becoming popular alternatives.<sup>14,15</sup> The reasons are varied, and certainly include the increasing chemical variety of non-natural building blocks being commercially available, the easy and modular nature of solid-phase peptide synthesis, and the inherent biocompatibility and potential biodegradability. The values of the energy band gap, calculated as the difference between the highest occupied molecular orbital (HOMO) and the lowest unoccupied molecular orbital (LUMO), can be even higher for peptide NTs relative to inorganic NTs (Fig. 1), demonstrating their high potential for uses in bioelectronics.<sup>16,17</sup>

Polypeptides' NTs were first reported using cyclic building blocks displaying alternating D- and L-amino acids by Ghadiri *et al.*,<sup>18</sup> and, in recent years, supramolecular alternatives using simpler building blocks are becoming attractive for their lower cost and simplicity of preparation. Amongst the various options, Phe-Phe NTs reported by Reches and Gazit<sup>19</sup> certainly stand out for robustness and interesting properties, and they are by far the most studied in this class.

### Phe-Phe nanotubes (NTs) structure and properties

The Phe-Phe NT characteristic architecture features an inner hydrophilic cavity enclosed by six peptide molecules positioned in alternating planes and interacting head-to-tail, with peptide stacks held together by intermolecular H-bonds between amide groups.<sup>20</sup> Remarkably, this structure revealed by single-crystal X-ray diffraction (XRD) data, was shown to correspond to that



Prof. Silvia Marchesan did her PhD at The University of Edinburgh (2008, UK), and postdoc research at the University of Helsinki (Finland), Monash University, and CSIRO (Melbourne, Australia). In 2013 she moved to the Center of Excellence for Nanostructured Materials at the University of Trieste (Italy) and she opened there the Superstructures Lab (<https://www.marchesanlab.com>) in 2015. In 2018, she became associate professor, got

habilitated as full professor, and was selected by Nature Index as Rising Star in the natural sciences. In 2021–2022 (6 months) she has been Visiting Professor at the University of Cambridge (UK), Yusuf Hamied Department of Chemistry.

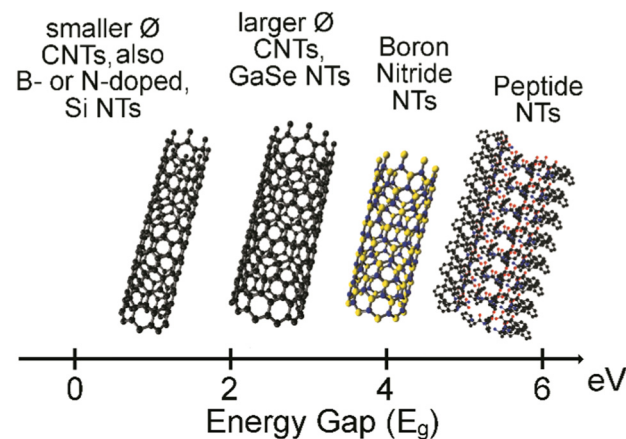


Fig. 1 HOMO–LUMO energy band gap in electronvolt (eV) for CNTs, inorganic NTs, and peptide NTs.<sup>16,17</sup>

found in the NTs, as confirmed by spectral matching with powder XRD data of the NTs.<sup>21</sup>

Phe-Phe NTs have been shown to be composed of nanocrystalline regions, which behave as quantum dots, as they display quantum confinement and exciton formation and luminescence at room temperature.<sup>22</sup> Remarkably, the blue photoluminescence was maintained even after thermal dehydration above 140 °C into fibrils formed by their cyclic analogs. This behavior opens the avenue to their potential use in photonics and displays as non-toxic alternatives to luminescent materials.<sup>23</sup>

Another interesting feature is the light-induced ferroelectricity of Phe-Phe NTs. This phenomenon requires two essential features, which are spontaneous polarisation and the ability to switch between two states in an electric field. In particular, the H-bonding network between the termini of the dipeptide molecules within the NTs was shown to switch between the zwitterionic and neutral states. The process is aided by the photoluminescent character of the NTs, with excitation light inducing the reduction of the intrinsic polarisation field, indicating the phenomenon happens at the nanoscale.<sup>24</sup>

Phe-Phe NTs display high average point stiffness of 160 N m<sup>-1</sup> and Young's modulus of 19–27 GPa, being amongst the stiffest biological materials known to date.<sup>25,26</sup> The longitudinal rigidity has been attributed to the zipper-like arrangement of interlocked aromatic residues.<sup>27</sup> Indeed, addition of further aromatic units using β,β-diphenylalanine enabled an increase to ~70 GPa, which is comparable to aluminium.<sup>28</sup> Conversely, the transversal rigidity has been attributed to the mobile water molecules inside the channels, with higher values corresponding to water-filled NTs.<sup>29</sup> New advanced microscopy methods to measure piezoresponse, mechanical, and dielectric properties of dipeptide NTs at the nanoscale are continuously being developed.<sup>30</sup>

The inner content of water determines also the type of nanomorphology attained with Phe-Phe self-assembly that can be controlled by varying the amount of relative humidity.<sup>31</sup> Interestingly, recent *in silico* investigations have suggested that the inner water clusters can acquire polar and chiral properties as a result of their interactions with the walls of the Phe-Phe NTs,

which exert such effects thanks to their dipole-moments distribution.<sup>32</sup>

Phe-Phe NTs have also been shown to be able to reversibly switch between the NTs and nanovesicle morphologies, for instance by dilution and increased concentration, respectively.<sup>33</sup> The morphological conversions have been shown to follow the Ostwald's rule of stages, with coalescence of monomers into nuclei, which then undergo ripening into NTs, as shown with Boc-Phe-Phe.<sup>34</sup> Recent studies have unveiled how only certain peptide backbone conformations found in intermediate species are compatible with, and proceed towards, NT assembly.<sup>35</sup> The use of doping additives and solvent choice offer further means to control the final nanomorphology of Phe-Phe assemblies.<sup>36</sup>

### The role of water inside the channels

One of the fascinating features of this type of NTs is the nanotubular architecture that encloses water-filled channels. Two types of water molecules are present, *i.e.* those bound to the peptide walls of the channels, and those that are mobile in the inner cavity. The bound water molecules are necessary for the NTs' structural integrity, as the NTs collapse without them. Conversely, the mobile water molecules are responsible for the physical properties of the NTs. Interestingly, a recent study showed that there are two types of diffusion regimes, with small clusters (<5 molecules per unit cell) displaying a ballistic type, and larger clusters displaying a Fickian type. The water diffusion coefficient was measured experimentally and found to be within range with other solid materials (Table 1).<sup>37</sup>

The radial growth and elongation of NTs during Phe-Phe self-assembly could be imaged by using liquid-cell transmission electron microscopy (LCTEM), which enables high resolution observation of solvated nanomaterials.<sup>48</sup> TeraHertz spectroscopy revealed breathing motions of dipeptide sidechains within the NTs that can affect the NTs permeability to water through changes in both the pore diameter and the host-water potential.<sup>49</sup>

Water inside the channel was demonstrated to alter also the electronic properties of the peptide NTs, by reducing the band gap and increasing the probability of hopping, hence conductivity.<sup>50</sup> Furthermore, addition of water molecules to the inner cavity of Phe-Phe NTs causes splitting of the valence band, which corresponds to a redshift and splitting of a UV photoluminescence peak.<sup>51</sup>

**Table 1** Water diffusion coefficients ( $D$ ) in various materials. Adapted with permission from P. S. Zelenovskiy *et al.* *ACS Appl. Mater. Interfaces*, 2020, **12**, 27485. Copyright 2020 © American Chemical Society<sup>37</sup>

| Material                 | $D \times 10^{-10} \text{ m}^2 \text{ s}^{-1}$ | Channel $\varnothing$ nm | Temp. °C | Ref.      |
|--------------------------|--|--------------------------|----------|-----------|
| Phe-Phe NTs              | 1.3–3.0  | 1.0                      | 30–65    | 37        |
| Cyclo(WL) <sub>n</sub>   | 0.6–1.3  | 0.6–1.0                  | 37       | 38        |
| Cyclo(QaEa) <sub>4</sub> | 4.4  | 1.0                      | 25       | 39        |
| Gramicidin A             | 0.3  | 0.5                      | 27       | 40        |
| Aquaporin 1              | 4–8  | 1.0–1.2                  | RT       | 41        |
| Nafion                   | 0.1–19.2                                       | 3.2                      | 23–70    | 42 and 43 |
| Zeolites                 | 0.5–1.3  | 0.3–1.0                  | 25       | 44        |
| Hydroxyapatite           | 10   | 2.0–24.0                 | 37       | 45        |
| Bulk water               | 21–26  | n.a.                     | 25       | 41 and 46 |
| Carbon NTs               | 26–96  | 1.2–3.5                  | –8 to 22 | 47        |

Peptide-water interactions are also important in the initial stages of self-assembly to direct it towards different nanomorphologies.<sup>52</sup> Higher contents of free-water (*i.e.*, lower ionic strength, lower solute concentrations) lead to preferred NT formation over nanowires, with the former being held by stronger H-bonds between dipeptide termini, and being more thermodynamically stable.<sup>53</sup>

The loss of water can be detected by low-frequency Raman spectroscopy, as it decreases the effect that water molecules have on the coupling between dipeptides, with an increase in bandwidth and energy separation between characteristic double-peak signals in the spectra.<sup>54</sup> Water indeed plays a key role in the early nucleation stages of peptide self-assembly<sup>55,56</sup> and NT elongation.<sup>57</sup>

## Dipeptide NTs and their chemical structures

### L-Dipeptides without derivatisations

Görbitz first reported a series of hydrophobic L-dipeptide crystal structures featuring characteristic supramolecular nanotubes (Table 2). Interestingly, Val-Ala,<sup>58</sup> Ala-Val,<sup>59</sup> Ala-Ile, Ile-Ala, Val-Val, Val-Ile, Ile-Val,<sup>60</sup> and Val-Leu<sup>61</sup> had hydrophobic inner walls due to the presence of the amino acid sidechains (yellow cells in Table 2). The self-assembly of Ala-Val and Val-Ala into different nanomorphologies was studied by changing solvent systems.<sup>62</sup>

Conversely, Leu-Leu, Phe-Phe, Leu-Phe, Phe-Leu,<sup>20</sup> Ile-Leu,<sup>63</sup> (cyan cells in Table 2) and Phe-Trp<sup>64</sup> displayed hydrophilic inner walls defined by the peptide backbones, with the side-chains defining the hydrophobic exterior of the nanotubes. The differences in packing and H-bonding networks are described in a detailed review.<sup>65</sup> Trp-Tyr were also recently reported to form nanotubes, although no crystal structure was available.<sup>66</sup>

L-DOPA is another aromatic amino acid that has gained wide attention for its bioactivity, and inclusion into self-assembled nanostructures, as recently reviewed by Tomasini's group.<sup>67</sup> However, when Phe was substituted with L-DOPA in the dipeptides DOPA-DOPA, nanofibrillar soft materials were obtained, with no evidence for nanotubes with a distinct inner cavity.<sup>58</sup>

### L,D-Heterochiral dipeptides without derivatisations

Our group has developed expertise in the design of self-assembling minimalistic peptides whereby inclusion of L- and

**Table 2** Hydrophobic homochiral dipeptides forming nanotubes with hydrophobic (yellow) or hydrophilic (cyan) inner cavity defined by 4 (Ⓐ) or 6 (Ⓑ) dipeptide molecules.<sup>20,58–61,65,69–71</sup> Adapted from C. H. Görbitz et al., *Chem. Eur. J.* 2007, **13**, 1022, Copyright © 2007 WILEY-VCH Verlag GmbH & Co. KGaA, Weinheim<sup>65</sup>

| N-terminal Xaa | C-terminal Xaa |     |     |     |     |
|----------------|----------------|-----|-----|-----|-----|
|                | Ala            | Val | Ile | Leu | Phe |
| <b>Ala</b>     | No             | Ⓐ   | Ⓐ   | No  | No  |
| <b>Val</b>     | Ⓐ              | Ⓐ   | Ⓐ   | Ⓐ   | No  |
| <b>Ile</b>     | Ⓐ              | Ⓐ   | No  | Ⓐ   | No  |
| <b>Leu</b>     | No             | No  | No  | Ⓐ   | Ⓐ   |
| <b>Phe</b>     | No             | No  | No  | Ⓐ   | Ⓑ   |

D-amino acids at specific positions plays a key role. In the case of hydrophobic tripeptides, heterochiral sequences can display an amphipathic conformation with hydrophobic sidechains being exposed on the opposite side relative to the hydrophilic backbones.<sup>72</sup> These peptides can also form supramolecular hydrogels at physiological conditions that generally display good cytocompatibility *in vitro*, with further advantages such as the possibility to fine-tune their biodegradation rate,<sup>73</sup> and easily encode bioactive sequences to guide cell fate.<sup>74</sup>

Recently, we explored also the case of hydrophobic heterochiral dipeptides' self-assembly. In the case of D-Phe-L-Phe, surprisingly, NTs were formed with analogous architecture to the homochiral counterpart, and a water-filled inner cavity (Fig. 2). However, the differing stereoconfiguration of the heterochiral dipeptides, resulted in different spatial orientation of the sidechains, which could engage in intramolecular interactions at the expense of intermolecular ones. As a result, D-Phe-L-Phe formed 4 nm wide gelling nanotubes defined by two peptide layers, leading to transparent hydrogels with good cytocompatibility in cell culture. This is in marked contrast with the heterogeneous size distribution of NTs formed by homochiral Phe-Phe that display hierarchical bundling that proceeds uncontrolled, with detrimental effects for cytocompatibility.<sup>75</sup> Interestingly, substitution of 1 H with 1 atom of fluorine at the N-terminus did not impede NT formation, although it yielded to intermediate levels of bundling, depending on the position of fluorine on the aromatic ring.<sup>73</sup> By contrast, the use of fluorophenylalanine at the C-terminus completely altered the supramolecular packing, leading to amphipathic layers – as opposed to water-channels – as revealed by single-crystal XRD.<sup>76</sup>

Substitution of one Phe with one of the hydrophobic aliphatic amino acids led to NTs too. We did not include Ala in the studies because our objective was to attain supramolecular hydrogels, and already the dipeptides Val-Phe and Phe-Val were at the limit of minimum hydrophobicity to yield stable gels.<sup>77</sup> Studies of all the possible stereoisomer combinations of Xaa-Phe and Phe-Xaa (Xaa = Val, Ile, or Leu), revealed that heterochirality increased the dipeptides' hydrophobicity. This fact was confirmed by increased retention times at the HPLC<sup>77–79</sup> (which can be considered an experimental measure of

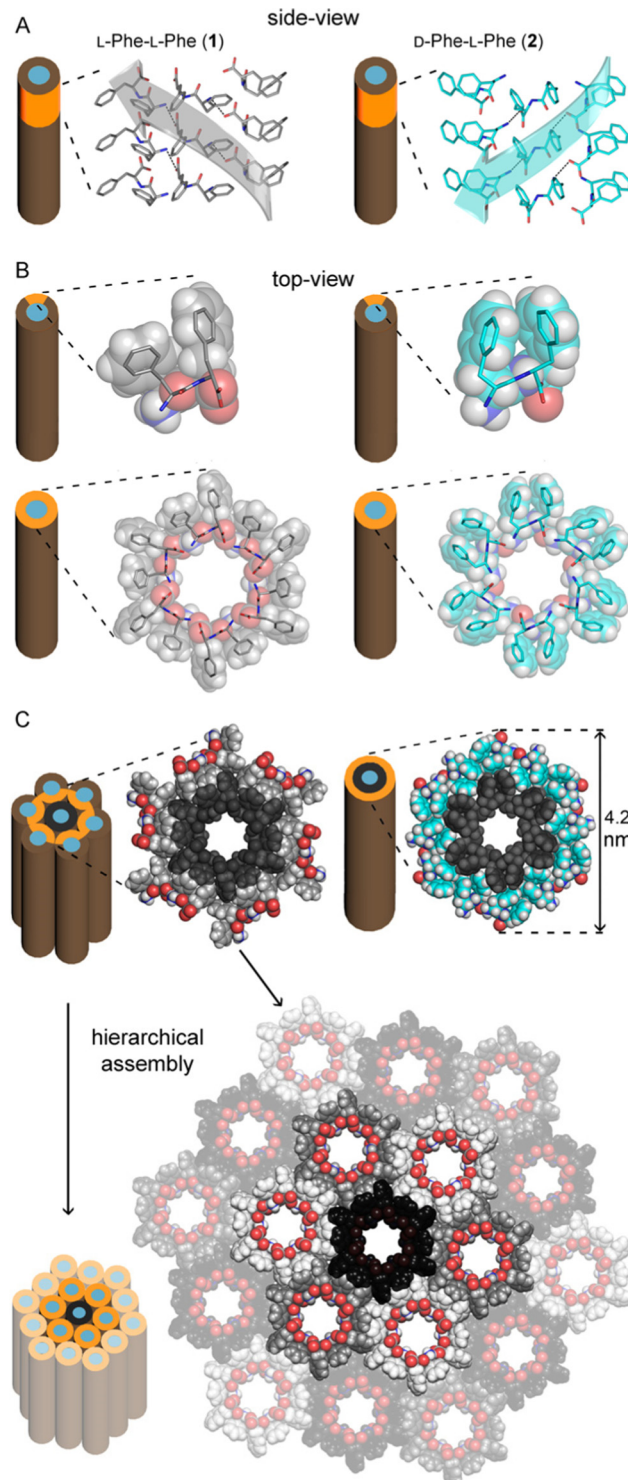


**Fig. 2** Single-crystal XRD structures of homochiral Phe-Phe<sup>20</sup> **1** (silver) and heterochiral D-Phe-L-Phe **2** (cyan) NTs. (A) Side-view of stacked peptides revealed opposite screw-sense for **1** and **2**, dictated by the chirality of the N-terminal amino acids. (B) Top-view of nanotube inner cavities defined by the projection of six peptide molecules arranged head-to-tail for both **1** and **2**. (C) Top-view of the nanotubes identified by the projection of 18 peptide molecules for **1** showed hierarchical bundling stabilized by aromatic zippers; instead, a space-fill view of heterochiral **2** revealed the outer diameter of a double layer of peptide molecules to agree with the diameter of fibrils measured by TEM.<sup>75</sup>

**Table 3** Heterochiral hydrophobic dipeptides forming NTs with water-filled internal cavities (cyan cells) defined by 4 (④) or 6 (⑥) peptide molecules.<sup>77–79</sup> “–” means no data is available

| N-terminal Xaa | C-terminal Xaa |     |     |     |
|----------------|----------------|-----|-----|-----|
|                | Val            | Ile | Leu | Phe |
| Val            | -              | -   | -   | No  |
| Ile            | -              | -   | -   | No  |
| Leu            | -              | -   | -   | No  |
| Phe            | ④              | ⑥   | -   | ⑥   |

hydrophobicity).<sup>80</sup> Furthermore, the formation of water-filled channels by heterochiral Phe-Xaa sequences (cyan cells in Table 3) was supported by single-crystal XRD. Interestingly, those formed by D-Phe-L-Val featured a smaller inner cavity ( $\sim 0.5$  nm) defined by four peptide molecules.<sup>77</sup> Conversely, the NTs formed by D-Phe-L-Ile or by D-Phe-L-Phe featured a larger inner cavity ( $\sim 1.0$  nm) defined by six dipeptide molecules.<sup>75,79</sup> Therefore, it is possible to fine-tune the water-channel cavity by choosing differing peptide sequences. All these sequences gelled, but over various timescales eventually converted into crystals. Furthermore, they displayed good cytocompatibility *in vitro* as assessed by MTT metabolic assays and by live/dead assays (Fig. 3), but already after 24 hours the gels has partially dissolved, thus suggesting limited durability for practical use in cell culture.<sup>81</sup> Noteworthily, the linear analog of Val (*i.e.*, norvaline, Nva) in homo- and heterochiral Nva-Phe and Phe-Nva sequences, led in all cases to immediate crystallization in phosphate buffered solutions, and single-crystal XRD revealed an amphipathic layered packing devoid of channels.<sup>82</sup> Ongoing studies in our laboratories are targeting the non-aromatic dipeptides of Table 3, for which no data is currently available pertaining their ability to form supramolecular channels, so as to provide a more complete picture.

### N-Capped dipeptides

Various N-terminal caps, such as acetylation, were shown to enable Phe-Phe self-assembly into NTs.<sup>83</sup> Boc-Phe-Phe can self-assemble into nanospheres or NTs depending on the solvents used, and the NTs can be inkjet printed to attain micropatterns.<sup>84</sup> Boc-Phe-Phe NTs were also embedded in electrospun polymer fibers to maximise their piezoelectric response for biosensing and bioelectronic applications.<sup>85</sup> Interestingly, the extent of the piezoelectric response depends also on the NT diameter.<sup>86</sup> Adler-Abramovich *et al.* combined Boc-Phe-Phe with Phe-Phe into supramolecular copolymers to yield NTs whose dimensions could be controlled by changing the ratios between the two building blocks.<sup>87</sup> Phe-Phe and Boc-Phe-Phe were also co-assembled into distinctive necklace nanoarchitectures as described by Reches' group.<sup>88</sup>

Boc-Ile-Ile-OMe was shown to self-assemble into NTs in methanol-containing solutions, with Boc playing a key role in directing the formation of the NT morphology.<sup>89</sup> Likewise, a

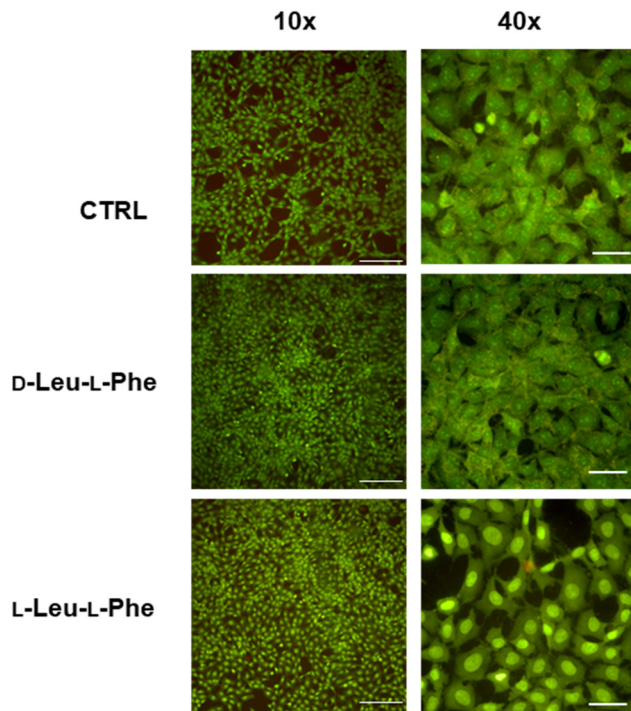


**Fig. 3** Live (green)/dead (red) assay for fibroblast cells grown for 24 hours on dipeptide hydrogels revealed excellent cell viability but also dissolution of the hydrogels. Scalebars = 200  $\mu$ m (10 $\times$ ) or 50  $\mu$ m (40 $\times$ ).<sup>81</sup>

work led by Moretto reported NTs formed by Boc-Cys(Me)-Leu-OMe.<sup>90</sup> One year later, NTs by Boc-Val-Ile-OMe, Boc-Val-Leu-OMe, Boc-Leu-Val-OMe, and Boc-Val-Val-OMe were described in solvent-water mixtures.<sup>91</sup> Finally, heterochiral Boc-D-Leu-L-Leu-OMe and Boc-D-allo-L-Ile-OMe also formed NTs with 6-fold symmetry analogously to Phe-Phe.<sup>92</sup>

Co-assembly of Fmoc-Phe-Phe with a phthalocyanine derivative resulted in the formation of helical NTs of 10–15 nm-diameter, depending on experimental conditions, which displayed intense circularly polarized luminescence. The authors envisaged potential applications in biomedicine or photocatalysis.<sup>93</sup> Fmoc-Lys-Phe-OMe was also reported to self-assemble into NTs when templated by addition of anionic heparin.<sup>94</sup>

Phe-Phe has been N-capped with chromophores Cy-3 and Cy-5 to form NTs that accumulated selectively in the mitochondria of human-carcinoma cells, whose extremely negative inner membrane potential [ $(\Delta\Psi_m)_{\text{cancer}} \approx -220$  mV] enabled their assembly leading to apoptosis.<sup>95</sup> These NTs could thus be useful for theranostics, thanks to combined imaging and therapeutic activity.

Fmoc-Lys-Lys has been covalently functionalized on the amino sidechain with 5-fluorouracil to yield a hydrogel composed of 16 nm wide nanotubes, with 4 nm thick walls featuring a bylayered structure composed of two dipeptide molecules. The hydrogel enabled the anti-metabolite drug sustained release and displayed no cytotoxicity *in vitro*.<sup>96</sup>

Naphthalimide N-capped Phe-Tyr was recently shown to yield NTs too. In this case, a phosphorylated precursor was used to control self-assembly triggered by phosphatase-catalysed enzymatic hydrolysis. The NTs formed a luminescent hydrogel.<sup>97</sup>

## Dehydro ( $\Delta$ ) dipeptides

Dehydro ( $\Delta$ ) amino acids display a double C=C bond between C $\alpha$  and C $\beta$  that restricts conformational freedom to enable the design of foldamers. Introduction of hydrophobic  $\Delta$  residues in Pro-containing dipeptide sequences was found to influence turn conformations and their stability, which was reduced with increasing solvent polarity.<sup>98</sup> In particular, the study of Ac-Pro- $\Delta$ Xaa-NHCH<sub>3</sub> revealed a tendency to adopt a  $\beta$ -turn in the decreasing order (Z)- $\Delta$ Abu > (E)- $\Delta$ Abu >  $\Delta$ Val, with  $\Delta$ Ala not displaying such tendency. Furthermore, none of the folds was stable in strongly solvating media.<sup>99</sup> Circular dichroism analysis of Phe- $\Delta$ Phe revealed a spectroscopic signature compatible with  $\beta$ -turns, and it formed proteolytically stable NTs. However, single-crystal XRD analyses revealed fine details over the supramolecular packing that was markedly different from Phe-Phe.<sup>100</sup>

The dipeptide based on Phe and its dehydroanalogs,  $\Delta$ Phe, was used for similar applications as Phe-Phe NTs, as it maintained the ability to form NTs that were then loaded with the tumor-specific testis-cancer antigen MAGE-3 to enable its delivery for cancer immunotherapy. The NTs demonstrated good stability against protease-mediated hydrolysis, they accumulated into antigen-presenting-cells and successfully elicited T-cell activation and tumor inhibition *in vivo*.<sup>101</sup> Phe- $\Delta$ Phe NTs were used also for the loading and release of curcumin as a model drug. Interestingly, simple variations of the sequence to Arg- $\Delta$ Phe, Val- $\Delta$ Phe, or Met- $\Delta$ Phe, hampered the NT formation in favour of spherical nanomorphologies.<sup>102</sup>

## $\beta$ - and $\gamma$ -dipeptides

$\beta$ - and  $\gamma$ -amino acids are characterized by one or two additional carbon atoms, respectively, between the amino and carboxylic functional groups. The position of the sidechain then determines the type of regioisomer, and the nomenclature of widely studied  $\beta$ -amino acids is reported in Fig. 4.<sup>103</sup> Certain  $\beta$ -amino acids occur in nature as secondary metabolites or components of natural products.<sup>104,105</sup> Amongst them,  $\beta$ -alanine is the most studied, and it occurs in natural bioactive dipeptides, such as carnosine.<sup>106</sup> Self-assembly of this dipeptide was achieved when using more hydrophobic derivatives.<sup>107,108</sup>  $\beta$ -Phe- $\Delta$ -Phe was designed to introduce flexibility at the N-terminus and

rigidity at the C-terminus. This dipeptide maintained the ability of parent Phe-Phe to self-assemble into NTs, although with a different supramolecular packing that defined water channels of  $\sim 0.5$  nm in diameter with crystalline water inside. This nanomaterial was envisaged for drug delivery, thanks to its proteolytic stability and ability to encapsulate drugs (*i.e.*, riboflavin, doxorubicin, chloroquine and chloramphenicol) without cytotoxicity *in vitro*.<sup>109</sup>

Hybrid  $\beta,\alpha$ -dipeptides featuring hydrophobic residues, and, in particular, a  $\beta$ -Ala at the N-terminus, followed by an  $\alpha$ -amino acid (*i.e.*, Phe, Ile, or Val) were reported to form NTs too, with good thermal and proteolytic stability.<sup>110</sup> These NTs were used as scaffolds for the *in situ* production of gold nanoparticles on their surface.<sup>110</sup> Alternatively, the decoration of  $\beta$ -Ala- $\alpha$ -Ile with fluorescent Au<sub>25</sub> quantum clusters was exploited to the same end, by using electron-beam irradiation as a means to control the gold-nanoparticle growth and size distribution.<sup>111</sup>

By contrast, when both residues of hydrophobic dipeptides were composed of  $\beta$ - or  $\gamma$ -amino acids (*i.e.*, Boc- $\beta^3(R)$ Phe- $\beta^3(R)$ Phe and Boc- $\gamma^4(R)$ Phe- $\gamma^4(R)$ Phe) NTs were not formed, and other morphologies could be attained depending on experimental conditions, and including nanofibers and nanospheres.<sup>112</sup>

The dipeptide displaying Ala and the *S,S* (but not the *R,R*) stereoisomer of 3-amino-2-(2-fluorophenyl)-3-phenylpropanoic acid was shown to self-assemble into proteolytically stable NTs, thanks to the presence of the  $\beta$ -amino acid. Interestingly, the XRD structure of this dipeptide revealed a supramolecular helix with three peptide molecules per turn, with the screw axis corresponding to the crystallographic *c* axis. These NTs featured a hydrophobic inner channel with a diameter of 4 Å that was decorated by the methyl sidechains. No evidence for aromatic stacking was found in the crystal structure, suggesting that intermolecular H-bonds proved key in holding the NT architecture.<sup>113</sup> Finally, also  $\beta$ -Ala-Ala and  $\delta$ -Ava-Phe (Ava = aminovaleric acid) were reported to self-assemble into NTs.<sup>114</sup>

## $\delta$ -Amino acids as dipeptide mimics and $\delta$ -dipeptides

$\delta$ -Amino acids are characterised by four atoms (typically carbon) between the amino and carboxylic functionalities and are seldom studied, possibly because of the synthetic steps needed and their limited solubility in water. They have been proposed as dipeptide mimics. In particular,  $\beta$ -Oxy- $\delta^5$ -amino acids bear an oxygen atom in their backbone that improves their solubility.<sup>115</sup> Inclusion of a cycle proved to be a successful strategy to restrict conformational freedom towards foldamers.<sup>116,117</sup> The combination of both components in cyclohexyl ether  $\delta$ -amino acids was successfully applied in building blocks to attain supramolecular channels with cation selectivity, thanks to the strategic disposition of the additional oxygen atom in the channel interior.<sup>118</sup>

## Cyclodipeptides (CDPs)

CDPs have attracted attention as building blocks for biocompatible nanostructures, since they are naturally occurring in a variety of food and beverages, and their rigidity and enhanced stability towards enzymatic degradation relative to their linear

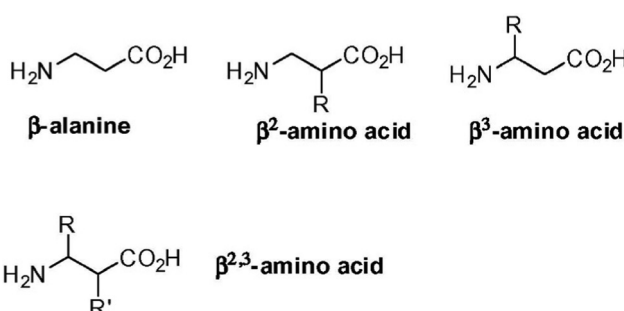


Fig. 4 Nomenclature of  $\beta$ -amino acids. Reprinted from F. Clerici, E. Erba, M. L. Gelmi and S. Pellegrino, *Tetrahedron Lett.*, 2016, **57**, 5540, Copyright © 2016, with permission from Elsevier.<sup>103</sup>

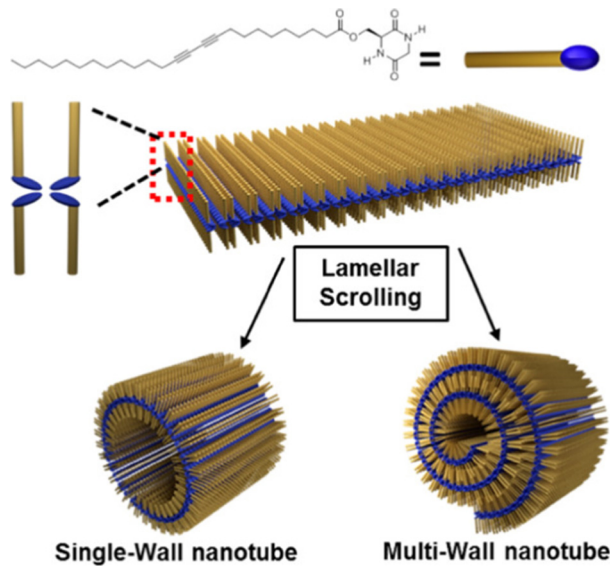


Fig. 5 Cyclodipeptide derivative with an alkyl chain enabled the formation of lamellar structures that rolled up into NTs. Reproduced with permission from M. J. Seo *et al.* *Langmuir*, 2018, **34**, 8365, Copyright © 2018, American Chemical Society.<sup>122</sup>

analogs, has enabled their use towards supramolecular nanostructures and soft materials for a variety of applications, as recently reviewed.<sup>119,120</sup> NTs and microtubes were reported for homochiral and heterochiral cyclo(Tyr-Ala), respectively.<sup>121</sup>

A different assembly was obtained using cyclodipeptides (CDPs) derivatised with long alkyl chains displaying photopolymerizable diacetylene functionalities for thermochromism and enable a lamellar structure to arise that rolled up into nanotubes (Fig. 5).<sup>122</sup> Interestingly, these systems displayed a blue-to-red thermochromism upon heating from room temperature to 90 °C. Furthermore, appropriate choice of solvent polarity could be exploited to guide self-assembly towards different nanomorphologies.<sup>123</sup>

Cyclo(Gly-Asp) amidated through the sidechain with a long alkyl chain (C<sub>8</sub>–C<sub>18</sub>) self-assembled into various nanomorphologies, including NTs that were envisaged for drug loading and release, and studied for their co-assembly ability with nucleoside biomolecules.<sup>124</sup>

### Dipeptides with non-natural aromatic structures

The key role played by the aromatic sidechains of Phe-Phe in the stability and physicochemical properties of the NTs<sup>125</sup> has inspired the search for several analogs with differing aromatic moieties. Interestingly, the simple removal of the methylene units leading to Phg-Phg (Phg = phenylglycine), with the phenyl ring being directly attached to the peptide backbone, completely hindered the NT formation, leading to nanospherical morphologies instead.<sup>126</sup> Conversely, dinaphthylalanine formed NTs,<sup>127</sup> as well as Boc-Aib-*m*-ABA-OMe (Aib =  $\alpha$ -aminoisobutyric acid; *m*-ABA = *m*-aminobenzoic acid).<sup>128</sup> 4'-(*n*-dodecyloxy)-1,1'-biphenyl-4-carbonyl Ala-Ala homo- and heterochiral isomers formed coiled nanoribbons that gave rise to NTs. Interestingly, the

stereoconfiguration of the C-terminal Ala residue dictated the handedness of the coiled nanoribbons, and the stacking handedness of the biphenylene moiety. Conversely, the N-terminal Ala chirality determined the twist handedness of the aromatic groups.<sup>129</sup> Another study showed that NTs with 6-fold symmetry could be obtained from the self-assembly of Boc-(*S,S*)-c<sub>3</sub>diPhe-(*R,R*)-c<sub>3</sub>diPhe-NH<sup>i</sup>Pr, which is a dipeptide with disubstituted cyclopropyl sidechains with two phenyl rings each.<sup>130</sup> This peculiar structure enabled the display of one of the aromatic units for each dipeptide in the inner cavity of the NT, in striking contrast with the typical NT architectures that feature hydrophilic peptide backbone at the NT interior and hydrophobic sidechains at the exterior.

### Applications

Clearly dipeptide NTs are ideally positioned for biological uses, spanning from drug delivery to cell culture and imaging. Control of self-assembly can be attained by using physiological or pathological triggers at the site of interest. A classical example is based on the enzymatic cleavage of a self-immolative unit, such as a dendrimer, to release the self-assembling dipeptide.<sup>131</sup> C-terminal amidation of Phe-Phe was used to yield a cationic dipeptide that at physiological pH could self-assemble into NTs that could bind the polyanionic oligonucleotides and that, contrarily to the zwitterionic Phe-Phe, transitioned to vesicles when diluted to 7 mg ml<sup>-1</sup>. The vesicles could then be taken up by cells for oligonucleotide delivery.<sup>132</sup> Flufenamic acid was used as a model drug that could be loaded in the hydrophobic walls of Phe-Phe NTs for sustained release over days.<sup>133</sup> Crosslinking with glutaraldehyde has been proposed as a strategy to control the nanoarchitectures formed by Phe-Phe for drug delivery.<sup>134</sup> The dipeptide Lys-Lys was conjugated through the amino side-chain to the anticancer drug camptothecin, which could be loaded at very high levels through hydrophobic interactions within the dipeptide NT walls, and slowly released through hydrolysis of a succinyl linker.<sup>135</sup> In a similar approach, double conjugation of Lys-Lys with camptothecin and 5-fluorouracil was used for the sequential release of the two drugs from the dipeptide NTs.<sup>136</sup> Alternatively, the inclusion of bioactive residues in dipeptides could also exert bioactivity, as demonstrated with L-DOPA in (*S*)-isopropyl 2-(2-amino-2-methylpropanamido)-3-(3,4-dihydroxyphenyl)propanoate that displayed anti-Parkinsonian activity in a rat model after oral administration.<sup>137</sup>

In light of the emergency we are facing in terms of emergence of antibiotic resistance, it is clear how the use of Phe-Phe NTs as antimicrobial agents is another hot topic. These NTs have been shown to eradicate Gram-positive bacterial biofilms, thanks to the formation of ion channels and/or surfactant-like activity, leading to biofilm matrix degradation and cell-membrane disruption, leading to cell death in *S. aureus* isolates.<sup>138</sup> They inhibited bacterial growth and led to cell death also of *E. coli*, thanks to an increase in cell membrane permeation and depolarization.<sup>139</sup>

Further applications can be envisaged by decorating the NTs with biomolecules, for instance as shown with biotin that was successfully recognized by avidin.<sup>140</sup> S-Glycosylation has also been explored as an avenue to fine-tune self-assembly of Phe-Phe.<sup>141</sup> For instance, addition of one, but not two, mannose units preserved Phe-Phe ability to form NTs, and recognition by lectins was envisaged to direct these materials towards biological use.<sup>142</sup>

Another growing field concerns bioelectronic applications towards sustainable and non-toxic alternatives to current systems in use. Several methods have been developed to orient and pattern dipeptide NTs into arrays for bioelectronics,<sup>143–147</sup> also on electrodes.<sup>148,149</sup> It was shown that even weak electric fields can facilitate the alignment of molecular dipole moments, accelerating the ordering of dipeptide and water molecules for self-assembly.<sup>150</sup> Alignment of Phe-Phe NTs is key to achieve unidirectional polarization and maximise their piezoelectric response for power generation, *i.e.*, for electrical energy production upon application of a mechanical force. Horizontally aligned Phe-Phe NT arrays have been used also as piezoelectric devices. Upon application of a force of 42 N, a peak voltage of 2.8 V was reached, with a current of 37.4 nA, and generated 8.2 nW that could power multiple liquid-crystal display panels.<sup>151</sup> For comparison, with an applied force of 60 N, vertically aligned Phe-Phe NTs generated an open-circuit voltage of 1.4 V with a short-circuit current of 39.2 nA.<sup>152</sup> Inclusion of porphyrins has been used as a strategy to slow down the biodegradation of Phe-Phe NTs in physiological conditions towards uses in implantable medical devices.<sup>153</sup>

The blue photoluminescence of dipeptide NTs has been envisaged as a biolabel, for applications in bioimaging and biosensing, thanks also to its persistence upon thermal treatment at temperatures in the 140–180 °C range, at which NTs undergo a transition to nanowires.<sup>154</sup> Their variations in photoluminescence have been applied for temperature sensing, with precision of 1 °C in the range 5–65 °C.<sup>155</sup> Dipeptide NTs have been studied also to develop biosensors for the electrochemical determination of dopamine.<sup>156</sup> They have been used as antennas or photosensitisers to enhance lanthanide luminescence for the detection of the neurotoxin paraoxon too.<sup>157</sup>

Phe-Phe microtubes have been envisaged also as optical waveguides, as demonstrated by illuminating one end of the microstructures and observing a bright spot of luminescence at the other end. However, for practical applications, further improvement to reduce attenuation through the length of the tubes are needed, possibly by improving the crystallinity or finding suitable derivatives.<sup>158,159</sup>

Finally, Phe-Phe NTs have been considered as nanofillers for biomedical materials, as they demonstrated to increase toughness and adhesive strength of epoxy resins, whilst preserving the elongation and thermal properties of the polymer matrix.<sup>160</sup>

## Conclusions and future perspectives

Dipeptide NTs have enjoyed two decades of intense research efforts worldwide since their early reports. Through the years, a

plethora of NT-forming dipeptides have been reported, and their biological uses have been envisaged through a variety of triggers to control the NT formation, their uptake by cells, and their release of bioactive compounds. The understanding of the key structural features of the dipeptides leading to NTs is still far from complete, however. Nevertheless, Görbitz made a tremendous effort to map the NTs architectures attained by simple hydrophobic L-dipeptides, showing that the aliphatic sequences yield NTs with hydrophobic interiors, whilst the aromatic ones tend to yield NTs with water-filled inner cavities. Changes in amino acid sequence can also be used to control the inner cavity diameter, as some preferentially form those enclosed by four dipeptides (leading to a cavity of ~0.5 nm), and others by six (leading to a cavity of ~1 nm). Bigger channels (*e.g.*, ~2 nm) can be attained by switching to tripeptides.<sup>161</sup> The control of NT growth for potential insertions into membranes could clearly open up new avenues, for instance to alter transport of guests selectively and find new means for therapeutic treatment.<sup>162</sup> Amongst the various approaches to control NT length, microfluidics is emerging as one possible strategy.<sup>163</sup> Alternatively, gases could be envisaged as channel guests, and one study appeared showing that porous dipeptide crystals have a remarkable selectivity for methane, carbon dioxide, and hydrogen absorption.<sup>164</sup>

Other areas of great interest pertain bioelectronics, to find sustainable and biodegradable alternatives to currently used components. A key challenge in this field is its highly multidisciplinary nature, which requires expertise in fields as diverse as engineering, photophysics, chemistry, and nanotechnology to make a qualitative leap. Nevertheless, the allure of being able one day to use biodegradable components for our everyday commodity devices is a great driver to innovate in this field and it is reasonable to expect that implementation into commercial devices is on its way to be soon realized on a large scale for the benefit of society.

## Author contributions

O. B. wrote the manuscript draft, under the supervision of P. D. A. and S. M. that guided the study, and revised the manuscript.

## Conflicts of interest

There are no conflicts to declare.

## Acknowledgements

The authors acknowledge the University of Trieste for providing a PhD scholarship to O. B. and funding to S. M. through FRA2022.

## Notes and references

- 1 S. Iijima, *Nature*, 1991, **354**, 56–58.

2 K. Aoki, N. Ogihara, M. Tanaka, H. Haniu and N. Saito, *J. Mater. Chem. B*, 2020, **8**, 9227–9238.

3 Z. Peng, T. Zhao, Y. Zhou, S. Li, J. Li and R. M. Leblanc, *Adv. Healthcare Mater.*, 2020, **9**, e1901495.

4 S. Marchesan, L. Ballerini and M. Prato, *Science*, 2017, **356**, 1010–1011.

5 L. Wieland, H. Li, C. Rust, J. Chen and B. S. Flavel, *Adv. Energy Mater.*, 2021, **11**, 2002880.

6 M. Melchionna and P. Fornasiero, *ChemCatChem*, 2017, **9**, 3274–3284.

7 D. Iglesias and M. Melchionna, *Catalysts*, 2019, **9**, 128.

8 Z. Xu, W. Deng and X. Wang, *Electrochem. Energy Rev.*, 2021, **4**, 269–335.

9 J. S. Bulmer, A. Kaniyoor and J. A. Elliott, *Adv. Mater.*, 2021, **33**, 2008432.

10 C. Liang, Y. Liu, W. Lu, G. Tian, Q. Zhao, D. Yang, J. Sun and D. Qi, *Nanoscale*, 2022, **14**, 3346–3366.

11 M. Serra, R. Arenal and R. Tenne, *Nanoscale*, 2019, **11**, 8073–8090.

12 D. Zhang, S. Zhang, N. Yapici, R. Oakley, S. Sharma, V. Parashar and Y. K. Yap, *ACS Omega*, 2021, **6**, 20722–20728.

13 M. Dai and R. Wang, *Small*, 2021, **17**, 2006813.

14 I. W. Hamley, *Angew. Chem., Int. Ed.*, 2014, **53**, 6866–6881.

15 Q. Song, Z. Cheng, M. Kariuki, S. C. L. Hall, S. K. Hill, J. Y. Rho and S. Perrier, *Chem. Rev.*, 2021, **121**, 13936–13995.

16 G. Praveena, P. Kolandaivel, N. Santhanamoorthi, V. Renugopalakrishnan and S. Ramakrishna, *J. Nanosci. Nanotechnol.*, 2007, **7**, 2253–2259.

17 N. Santhanamoorthi, P. Kolandaivel, L. Adler-Abramovich, E. Gazit, S. Filipek, S. Viswanathan, A. Strzelczyk and V. Renugopalakrishnan, *Adv. Mater. Lett.*, 2011, **2**, 100–105.

18 M. R. Ghadiri, J. R. Granja, R. A. Milligan, D. E. McRee and N. Khazanovich, *Nature*, 1993, **366**, 324–327.

19 M. Reches and E. Gazit, *Science*, 2003, **300**, 625–627.

20 C. H. Görbitz, *Chem. – Eur. J.*, 2001, **7**, 5153–5159.

21 C. H. Görbitz, *Chem. Commun.*, 2006, 2332–2334.

22 N. Amdursky, P. Beker, I. Koren, B. Bank-Srour, E. Mishina, S. Semin, T. Rasing, Y. Rosenberg, Z. Barkay, E. Gazit and G. Rosenman, *Biomacromolecules*, 2011, **12**, 1349–1354.

23 A. Handelman, A. Natan and G. Rosenman, *J. Pept. Sci.*, 2014, **20**, 487–493.

24 Z. Gan, X. Wu, X. Zhu and J. Shen, *Angew. Chem., Int. Ed.*, 2013, **52**, 2055–2059.

25 N. Kol, L. Adler-Abramovich, D. Barlam, R. Z. Shneck, E. Gazit and I. Roussel, *Nano Lett.*, 2005, **5**, 1343–1346.

26 L. Niu, X. Chen, S. Allen and S. J. Tendler, *Langmuir*, 2007, **23**, 7443–7446.

27 I. Azuri, L. Adler-Abramovich, E. Gazit, O. Hod and L. Kronik, *J. Am. Chem. Soc.*, 2014, **136**, 963–969.

28 V. Basavalingappa, S. Bera, B. Xue, J. O'Donnell, S. Guerin, P. A. Cazade, H. Yuan, E. U. Haq, C. Silien, K. Tao, L. J. W. Shimon, S. A. M. Tofail, D. Thompson, S. Kolusheva, R. Yang, Y. Cao and E. Gazit, *ACS Nano*, 2020, **14**, 7025–7037.

29 P. Zelenovskiy, I. Kornev, S. Vasilev and A. Kholkin, *Phys. Chem. Chem. Phys.*, 2016, **18**, 29681–29685.

30 A. Kalinin, V. Atepalkhin, O. Pakhomov, A. L. Kholkin and A. Tselev, *Ultramicroscopy*, 2018, **185**, 49–54.

31 M. Wang, L. Du, X. Wu, S. Xiong and P. K. Chu, *ACS Nano*, 2011, **5**, 4448–4454.

32 V. S. Bystrov and S. V. Filippov, *J. Mol. Model.*, 2022, **28**, 81.

33 X. Yan, Y. Cui, Q. He, K. Wang, J. Li, W. Mu, B. Wang and Z. C. Ou-Yang, *Chem. – Eur. J.*, 2008, **14**, 5974–5980.

34 A. Levin, T. O. Mason, L. Adler-Abramovich, A. K. Buell, G. Meisl, C. Galvagnion, Y. Bram, S. A. Stratford, C. M. Dobson, T. P. Knowles and E. Gazit, *Nat. Commun.*, 2014, **5**, 5219.

35 Q. Xiong, Y. Jiang, X. Cai, F. Yang, Z. Li and W. Han, *ACS Nano*, 2019, **13**, 4455–4468.

36 A. C. C. Ribeiro, G. A. Souza, D. H. Pereira, D. S. Cordeiro, R. S. Miranda, R. Custódio and T. D. Martins, *ACS Omega*, 2019, **4**, 606–619.

37 P. S. Zelenovskiy, E. M. Domingues, V. Slabov, S. Kopyl, V. L. Ugolkov, F. M. L. Figueiredo and A. L. Kholkin, *ACS Appl. Mater. Interfaces*, 2020, **12**, 27485–27492.

38 J. Liu, J. Fan, M. Tang, M. Cen, J. Yan, Z. Liu and W. Zhou, *J. Phys. Chem. B*, 2010, **114**, 12183–12192.

39 M. Engels, D. Bashford and M. R. Ghadiri, *J. Am. Chem. Soc.*, 1995, **117**, 9151–9158.

40 S. W. Chiu, E. Jakobsson, S. Subramaniam and J. A. McCammon, *Biophys. J.*, 1991, **60**, 273–285.

41 J. B. Heymann and A. Engel, *News Physiol. Sci.*, 1999, **14**, 187–193.

42 Q. Zhao, P. Majsztrik and J. Benziger, *J. Phys. Chem. B*, 2011, **115**, 2717–2727.

43 S. J. Paddison and R. Paul, *Phys. Chem. Chem. Phys.*, 2002, **4**, 1158–1163.

44 T. Yamamoto, Y. H. Kim, B. C. Kim, A. Endo, N. Thongprachan and T. Ohmori, *Chem. Eng. J.*, 2012, **181–182**, 443–448.

45 T. Honório, T. Lemaire, D. D. Tommaso and S. Naili, *Comput. Mater. Sci.*, 2019, **156**, 26–34.

46 J. H. Wang, *J. Phys. Chem.*, 1965, **69**, 4412.

47 J. Hassan, G. Diamantopoulos, L. Gkoura, M. Karagianni, S. Alhassan, S. V. Kumar, M. S. Katsiotis, T. Karagiannis, M. Fardis, N. Panopoulos, H. J. Kim, M. Beazi-Katsioti and G. Papavassiliou, *J. Phys. Chem. C*, 2018, **122**, 10600–10606.

48 K. Gnanasekaran, J. Korpanty, O. Berger, N. Hampu, M. Halperin-Sternfeld, D. Cohen-Gerassi, L. Adler-Abramovich and N. C. Gianneschi, *ACS Nano*, 2021, **15**, 16542–16551.

49 H. Zhang, K. Siegrist, D. F. Plusquellec and S. K. Gregurick, *J. Am. Chem. Soc.*, 2008, **130**, 17846–17857.

50 T. Andrade-Filho, F. F. Ferreira, W. A. Alves and A. R. Rocha, *Phys. Chem. Chem. Phys.*, 2013, **15**, 7555–7559.

51 M. Wang, S. Xiong, X. Wu and P. K. Chu, *Small*, 2011, **7**, 2801–2807.

52 C. Guo, Y. Luo, R. Zhou and G. Wei, *ACS Nano*, 2012, **6**, 3907–3918.

53 J. Kim, T. H. Han, Y. I. Kim, J. S. Park, J. Choi, D. G. Churchill, S. O. Kim and H. Ihhee, *Adv. Mater.*, 2010, **22**, 583–587.

54 X. Wu, S. Xiong, M. Wang, J. Shen and P. K. Chu, *Opt. Express*, 2012, **20**, 5119–5126.

55 J. Wang, C. Yuan, Y. Han, Y. Wang, X. Liu, S. Zhang and X. Yan, *Small*, 2017, **13**, 1702175.

56 J. Anderson, P. T. Lake and M. McCullagh, *J. Phys. Chem. B*, 2018, **122**, 12331–12341.

57 J. Wang, K. Liu, L. Yan, A. Wang, S. Bai and X. Yan, *ACS Nano*, 2016, **10**, 2138–2143.

58 C. H. Görbitz and E. Gundersen, *Acta Crystallogr., Sect. C: Cryst. Struct. Commun.*, 1996, **52**, 1764–1767.

59 C. H. Görbitz, *Acta Crystallogr., Sect. B: Struct. Sci.*, 2002, **58**, 849–854.

60 C. H. Görbitz, *New J. Chem.*, 2003, **27**, 1789–1793.

61 C. H. Görbitz, *Acta Crystallogr., Sect. B: Struct. Sci., Cryst. Eng. Mater.*, 2018, **74**, 311–318.

62 H. Erdogan, E. Babur, M. Yilmaz, E. Candas, M. Gordesel, Y. Dede, E. E. Oren, G. B. Demirel, M. K. Ozturk, M. S. Yavuz and G. Demirel, *Langmuir*, 2015, **31**, 7337–7345.

63 C. Görbitz and E. Gundersen, *Acta Chem. Scand.*, 1996, **50**, 537–543.

64 C. Görbitz, *Acta Crystallogr., Sect. C: Cryst. Struct. Commun.*, 2006, **62**, o328–o330.

65 C. H. Görbitz, *Chem. – Eur. J.*, 2007, **13**, 1022–1031.

66 P. Macha, L. Perreault, Y. Hamedani, M. L. Mayes and M. C. Vasudev, *ACS Appl. Bio Mater.*, 2018, **1**, 1266–1275.

67 D. Giuri, P. Ravarino and C. Tomasini, *Org. Biomol. Chem.*, 2021, **19**, 4622–4636.

68 G. Fichman, L. Adler-Abramovich, S. Manohar, I. Mironi-Harpaz, T. Guterman, D. Seliktar, P. B. Messersmith and E. Gazit, *ACS Nano*, 2014, **8**, 7220–7228.

69 C. H. Görbitz, *Acta Crystallogr., Sect. C: Cryst. Struct. Commun.*, 2004, **60**, o371–o373.

70 R. J. Fletterick, C. C. Tsai and R. E. Hughes, *J. Phys. Chem.*, 1971, **75**, 918–922.

71 C. Görbitz, *Acta Crystallogr., Sect. E: Struct. Rep. Online*, 2004, **60**, o647–o650.

72 A. V. Vargiu, D. Iglesias, K. E. Styan, L. J. Waddington, C. D. Easton and S. Marchesan, *Chem. Commun.*, 2016, **52**, 5912–5915.

73 S. Marchesan, K. E. Styan, C. D. Easton, L. Waddington and A. V. Vargiu, *J. Mater. Chem. B*, 2015, **3**, 8123–8132.

74 M. C. Cringoli, C. Romano, E. Parisi, L. J. Waddington, M. Melchionna, S. Semeraro, R. De Zorzi, M. Grönholm and S. Marchesan, *Chem. Commun.*, 2020, **56**, 3015–3018.

75 S. Kralj, O. Bellotto, E. Parisi, A. M. Garcia, D. Iglesias, S. Semeraro, C. Deganutti, P. D'Andrea, A. V. Vargiu, S. Geremia, R. De Zorzi and S. Marchesan, *ACS Nano*, 2020, **14**, 16951–16961.

76 E. Scarel, O. Bellotto, P. Rozhin, S. Kralj, M. Tortora, A. V. Vargiu, R. De Zorzi, B. Rossi and S. Marchesan, *Soft Matter*, 2022, **18**, 2129–2136.

77 O. Bellotto, G. Pierri, P. Rozhin, M. Polentarutti, S. Kralj, P. D'Andrea, C. Tedesco and S. Marchesan, *Org. Biomol. Chem.*, 2022, **20**, 6211–6218.

78 O. Bellotto, S. Kralj, R. De Zorzi, S. Geremia and S. Marchesan, *Soft Matter*, 2020, **16**, 10151–10157.

79 O. Bellotto, S. Kralj, M. Melchionna, P. Pengo, M. Kisovec, M. Podobnik, R. De Zorzi and S. Marchesan, *ChemBioChem*, 2022, **23**, e202100518.

80 H. L. Bolt, C. E. J. Williams, R. V. Brooks, R. N. Zuckermann, S. L. Cobb and E. H. C. Bromley, *Biopolymers*, 2017, **108**, e23014.

81 O. Bellotto, PhD thesis, University of Trieste, 2022.

82 E. Scarel, G. Pierri, P. Rozhin, S. Adorinni, M. Polentarutti, C. Tedesco and S. Marchesan, *Chemistry*, 2022, **4**, 1417–1428.

83 M. Reches and E. Gazit, *Isr. J. Chem.*, 2005, **45**, 363–371.

84 L. Adler-Abramovich and E. Gazit, *J. Pept. Sci.*, 2008, **14**, 217–223.

85 R. M. F. Baptista, E. de Matos Gomes, M. M. M. Raposo, S. P. G. Costa, P. E. Lopes, B. Almeida and M. S. Belsley, *Nanoscale Adv.*, 2019, **1**, 4339–4346.

86 A. Kholkin, N. Amdursky, I. Bdikin, E. Gazit and G. Rosenman, *ACS Nano*, 2010, **4**, 610–614.

87 L. Adler-Abramovich, P. Marco, Z. A. Arnon, R. C. Creasey, T. C. Michaels, A. Levin, D. J. Scurr, C. J. Roberts, T. P. Knowles, S. J. Tendler and E. Gazit, *ACS Nano*, 2016, **10**, 7436–7442.

88 S. Yuran, Y. Razvag and M. Reches, *ACS Nano*, 2012, **6**, 9559–9566.

89 C. Subbalakshmi, S. V. Manorama and R. Nagaraj, *J. Pept. Sci.*, 2012, **18**, 283–292.

90 D. Mazzier, F. Carraro, M. Crisma, M. Rancan, C. Toniolo and A. Moretto, *Soft Matter*, 2016, **12**, 238–245.

91 C. Subbalakshmi, P. Basak and R. Nagaraj, *Biopolymers*, 2017, **108**, e23033.

92 B. Di Blasio, M. Saviano, V. Del Duca, G. De Simone, F. Rossi, C. Pedone, E. Benedetti and G. P. Lorenzi, *Biopolymers*, 1995, **36**, 401–408.

93 X. Wang, L. Zhao, C. Wang, X. Feng, Q. Ma, G. Yang, T. Wang, X. Yan and J. Jiang, *Small*, 2022, **18**, e2104438.

94 Y. M. Abul-Haija and R. V. Ulijn, *Biomacromolecules*, 2015, **16**, 3473–3479.

95 P. C. Saha, T. Bera, T. Chatterjee, J. Samanta, A. Sengupta, M. Bhattacharya and S. Guha, *Bi conjugate Chem.*, 2021, **32**, 833–841.

96 Y. Sun, J. A. Kaplan, A. Shieh, H. L. Sun, C. M. Croce, M. W. Grinstaff and J. R. Parquette, *Chem. Commun.*, 2016, **52**, 5254–5257.

97 R. D. Chakravarthy, M. Mohammed and H.-C. Lin, *Chem. – Asian J.*, 2020, **15**, 2696–2705.

98 M. Lisowski, G. Pietrzyński and B. Rzeszotarska, *Int. J. Pept. Protein Res.*, 1993, **42**, 466–474.

99 C. Pietrzyński, B. Rzeszotarska, E. Ciszak, M. Lisowski, Z. Kubica and G. Boussard, *Int. J. Pept. Protein Res.*, 1996, **48**, 347–356.

100 M. Gupta, A. Bagaria, A. Mishra, P. Mathur, A. Basu, S. Ramakumar and V. S. Chauhan, *Adv. Mater.*, 2007, **19**, 858–861.

101 P. Verma, S. Biswas, N. Yadav, A. Khatri, H. Siddiqui, J. J. Panda, B. S. Rawat, P. Tailor and V. S. Chauhan, *Mol. Pharming*, 2021, **18**, 3832–3842.

102 S. Alam, J. J. Panda, T. K. Mukherjee and V. S. Chauhan, *J. Nanobiotechnol.*, 2016, **14**, 26.

103 F. Clerici, E. Erba, M. L. Gelmi and S. Pellegrino, *Tetrahedron Lett.*, 2016, **57**, 5540–5550.

104 G. Lelais and D. Seebach, *Biopolymers*, 2004, **76**, 206–243.

105 F. Kudo, A. Miyanaga and T. Eguchi, *Nat. Prod. Rep.*, 2014, **31**, 1056–1073.

106 A. A. Boldyrev, G. Aldini and W. Derave, *Physiol. Rev.*, 2013, **93**, 1803–1845.

107 V. Castelletto, C. J. C. Edwards-Gayle, F. Greco, I. W. Hamley, J. Seitsonen and J. Ruokolainen, *ACS Appl. Mater. Interfaces*, 2019, **11**, 33573–33580.

108 V. Castelletto, G. Cheng, B. W. Greenland, I. W. Hamley and P. J. Harris, *Langmuir*, 2011, **27**, 2980–2988.

109 S. Parween, A. Misra, S. Ramakumar and V. S. Chauhan, *J. Mater. Chem. B*, 2014, **2**, 3096–3106.

110 S. Guha and A. Banerjee, *Adv. Funct. Mater.*, 2009, **19**, 1949–1961.

111 P. Ramasamy, S. Guha, E. S. Shibu, T. S. Sreeprasad, S. Bag, A. Banerjee and T. Pradeep, *J. Mater. Chem.*, 2009, **19**, 8456–8462.

112 B. Dinesh, M. A. Squillaci, C. Ménard-Moyon, P. Samori and A. Bianco, *Nanoscale*, 2015, **7**, 15873–15879.

113 A. Bonetti, S. Pellegrino, P. Das, S. Yuran, R. Bucci, N. Ferri, F. Meneghetti, C. Castellano, M. Reches and M. L. Gelmi, *Org. Lett.*, 2015, **17**, 4468–4471.

114 S. Guha, M. G. B. Drew and A. Banerjee, *Chem. Mater.*, 2008, **20**, 2282–2290.

115 R. M. Reja, R. Patel, V. Kumar, A. Jha and H. N. Gopi, *Biomacromolecules*, 2019, **20**, 1254–1262.

116 H.-D. Arndt, B. Ziemer and U. Koert, *Org. Lett.*, 2004, **6**, 3269–3272.

117 E. O'Reilly, L. Pes, Y. Ortin, H. Müller-Bunz and F. Paradisi, *Amino Acids*, 2013, **44**, 511–518.

118 H.-D. Arndt, A. Knoll and U. Koert, *Angew. Chem., Int. Ed.*, 2001, **40**, 2076–2078.

119 S. Manchineella and T. Govindaraju, *ChemPlusChem*, 2017, **82**, 88–106.

120 M. Scarel and S. Marchesan, *Molecules*, 2021, **26**, 3376.

121 A. Jeziorna, K. Stopczyk, E. Skorupska, K. Luberda-Durnas, M. Oszajca, W. Lasocha, M. Gorecki, J. Frelek and M. J. Potrzebowski, *Cryst. Growth Des.*, 2015, **15**, 5138–5148.

122 M. J. Seo, J. Song, C. Kantha, M. I. Khazi, U. Kundapur, J. M. Heo and J. M. Kim, *Langmuir*, 2018, **34**, 8365–8373.

123 M. I. Khazi, C. Balachandra, G. Shin, G. H. Jang, T. Govindaraju and J. M. Kim, *RSC Adv.*, 2020, **10**, 35389–35396.

124 K. Pandurangan, B. Roy, K. Rajasekhar, Y. V. Suseela, P. Nagendra, A. Chaturvedi, U. R. Satwik, N. A. Murugan, U. Ramamurty and T. Govindaraju, *ACS Appl. Bio Mater.*, 2020, **3**, 3413–3422.

125 L. Adler-Abramovich, M. Reches, V. L. Sedman, S. Allen, S. J. B. Tendler and E. Gazit, *Langmuir*, 2006, **22**, 1313–1320.

126 M. Reches and E. Gazit, *Nano Lett.*, 2004, **4**, 581–585.

127 V. L. Sedman, S. Allen, X. Chen, C. J. Roberts and S. J. Tendler, *Langmuir*, 2009, **25**, 7256–7259.

128 S. Kar and Y. Tai, *Soft Matter*, 2015, **11**, 1345–1351.

129 L. Zhang, J. Qin, S. Lin, Y. Li, B. Li and Y. Yang, *Langmuir*, 2017, **33**, 10951–10957.

130 M. Crisma, C. Toniolo, S. Royo, A. I. Jiménez and C. Catiuviela, *Org. Lett.*, 2006, **8**, 6091–6094.

131 L. Adler-Abramovich, R. Perry, A. Sagi, E. Gazit and D. Shabat, *ChemBioChem*, 2007, **8**, 859–862.

132 X. Yan, Q. He, K. Wang, L. Duan, Y. Cui and J. Li, *Angew. Chem., Int. Ed.*, 2007, **46**, 2431–2434.

133 T. Zohrabi, N. Habibi, A. Zarrabi, M. Fanaei and L. Y. Lee, *J. Biomed. Mater. Res., Part A*, 2016, **104**, 2280–2290.

134 A. Wu, Y. Guo, X. Li, Q. Li, G. Chen, H. Zang and J. Li, *J. Colloid Interface Sci.*, 2023, **630**, 161–169.

135 S. H. Kim, J. A. Kaplan, Y. Sun, A. Shieh, H. L. Sun, C. M. Croce, M. W. Grinstaff and J. R. Parquette, *Chem. – Eur. J.*, 2015, **21**, 101–105.

136 Y. Sun, C. M. Fry, A. Shieh, X. Cai, T. J. Reardon and J. R. Parquette, *Org. Biomol. Chem.*, 2022, **20**, 5254–5258.

137 T. Zhou, R. C. Hider, P. Jenner, B. Campbell, C. J. Hobbs, S. Rose, M. Jairaj, K. A. Tayarani-Binazir and A. Syme, *Bioorg. Med. Chem. Lett.*, 2013, **23**, 5279–5282.

138 S. L. Porter, S. M. Coulter, S. Pentlavalli, T. P. Thompson and G. Laverty, *Acta Biomater.*, 2018, **77**, 96–105.

139 L. Schnaider, S. Brahmachari, N. W. Schmidt, B. Mensa, S. Shaham-Niv, D. Bychenko, L. Adler-Abramovich, L. J. W. Shimon, S. Kolusheva, W. F. De Grado and E. Gazit, *Nat. Commun.*, 2017, **8**, 1–10.

140 M. Reches and E. Gazit, *J. Nanosci. Nanotechnol.*, 2007, **7**, 2239–2245.

141 R. Roytman, L. Adler-Abramovich, K. S. Kumar, T. C. Kuan, C. C. Lin, E. Gazit and A. Brik, *Org. Biomol. Chem.*, 2011, **9**, 5755–5761.

142 N. Gour, A. K. Barman and S. Verma, *J. Pept. Sci.*, 2012, **18**, 405–412.

143 L. Adler-Abramovich, D. Aronov, E. Gazit and G. Rosenman, *J. Nanosci. Nanotechnol.*, 2009, **9**, 1701–1708.

144 L. Adler-Abramovich, D. Aronov, P. Beker, M. Yevnin, S. Stempler, L. Buzhansky, G. Rosenman and E. Gazit, *Nat. Nanotechnol.*, 2009, **4**, 849–854.

145 J. Castillo, S. Tanzi, M. Dimaki and W. Svendsen, *Electrophoresis*, 2008, **29**, 5026–5032.

146 M. Reches and E. Gazit, *Nat. Nanotechnol.*, 2006, **1**, 195–200.

147 X. Liu, J. Danglad-Flores, S. Eickelmann, B. Sun, J. Hao, H. Riegler and J. Li, *ACS Nano*, 2022, **16**, 10372–10382.

148 L. Adler-Abramovich, M. Badihi-Mossberg, E. Gazit and J. Rishpon, *Small*, 2010, **6**, 825–831.

149 M. C. Vasudev, H. Koerner, K. M. Singh, B. P. Partlow, D. L. Kaplan, E. Gazit, T. J. Bunning and R. R. Naik, *Biomacromolecules*, 2014, **15**, 533–540.

150 C. M. Kelly, T. Northey, K. Ryan, B. R. Brooks, A. L. Kholkin, B. J. Rodriguez and N. V. Buchete, *Biophys. Chem.*, 2015, **196**, 16–24.

151 J. H. Lee, K. Heo, K. Schulz-Schönhagen, J. H. Lee, M. S. Desai, H. E. Jin and S. W. Lee, *ACS Nano*, 2018, **12**, 8138–8144.

152 V. Nguyen, R. Zhu, K. Jenkins and R. Yang, *Nat. Commun.*, 2016, **7**, 13566.

153 Y. Kim, H. Park, Y. Kim, C. Lee, H. Park and J.-H. Lee, *ACS Appl. Mater. Interfaces*, 2022, **14**, 38778–38785.

154 A. Handelman, N. Kuritz, A. Natan and G. Rosenman, *Langmuir*, 2016, **32**, 2847–2862.

155 Z. Gan, X. Wu, J. Zhang, X. Zhu and P. K. Chu, *Biomacromolecules*, 2013, **14**, 2112–2116.

156 O. Matos Ide and W. A. Alves, *ACS Appl. Mater. Interfaces*, 2011, **3**, 4437–4443.

157 J. H. Kim, J. Ryu and C. B. Park, *Small*, 2011, **7**, 718–722.

158 Q. Li, Y. Jia, L. Dai, Y. Yang and J. Li, *ACS Nano*, 2015, **9**, 2689–2695.

159 Q. Li, H. Ma, A. Wang, Y. Jia, L. Dai and J. Li, *Adv. Opt. Mater.*, 2015, **3**, 194–198.

160 N. Even, L. Adler-Abramovich, L. Buzhansky, H. Dodiuk and E. Gazit, *Small*, 2011, **7**, 1007–1011.

161 A. M. Garcia, D. Iglesias, E. Parisi, K. E. Stylian, L. J. Waddington, C. Deganutti, R. De Zorzi, M. Grassi, M. Melchionna, A. V. Vargiu and S. Marchesan, *Chem*, 2018, **4**, 1862–1876.

162 G. Picci, S. Marchesan and C. Caltagirone, *Biomedicines*, 2022, **10**, 885.

163 Z. A. Arnon, A. Vitalis, A. Levin, T. C. T. Michaels, A. Caflisch, T. P. J. Knowles, L. Adler-Abramovich and E. Gazit, *Nat. Commun.*, 2016, **7**, 13190.

164 A. Comotti, S. Bracco, G. Distefano and P. Sozzani, *Chem. Commun.*, 2009, 284–286.